Separation Science and Technology
Publication details, including instructions for authors and subscription information:
http://www.informaworld.com/smpp/title~content=t713708471

Fractionation of Pre-Hydrolysis Products from Lignocellulosic Biomass by an Ultrafiltration Ceramic Tubular Membrane

Kendra R. Colyar[a]; John Pellegrino[a]; Kiran Kadam[b]
[a] Department of Civil, Environmental, and Architectural Engineering, University of Colorado, Boulder, CO [b] PureVision Technology, Inc., Fort Lupton, CO

To cite this Article Colyar, Kendra R. , Pellegrino, John and Kadam, Kiran(2008) 'Fractionation of Pre-Hydrolysis Products from Lignocellulosic Biomass by an Ultrafiltration Ceramic Tubular Membrane', Separation Science and Technology, 43: 3, 447 — 476
To link to this Article: DOI: 10.1080/01496390701812517
URL: http://dx.doi.org/10.1080/01496390701812517

Separation Science and Technology, 43: 447–476, 2008

ISSN 0149-6395 print/1520-5754 online
DOI: 10.1080/01496390701812517

Fractionation of Pre-Hydrolysis Products from Lignocellulosic Biomass by an Ultrafiltration Ceramic Tubular Membrane

Kendra R. Colyar,[1] John Pellegrino,[1] and Kiran Kadam[2]

[1]Department of Civil, Environmental, and Architectural Engineering, University of Colorado, Boulder, CO
[2]PureVision Technology, Inc., Fort Lupton, CO

Abstract: Development of the lignocellulosic-biomass-based biorefinery for making transportation fuels requires the production of valuable byproducts, minimizing the chemical consumables, and efficient water recovery and reuse. Our focus is on a liquid stream containing a variety of soluble lignin species and alkalinity that is produced by a novel extrusion reactor that was used to break down corn stover to cellulose, sugar acids, and lignin. We report on the ambient temperature fractionation of this byproduct stream with a γ-alumina ceramic tubular membrane. There are four primary figures-of-merit investigated in this study: permeance decline, total organic carbon recovery (TOC) and sodium recovery, and the average molecular mass of organic compounds rejected and permeated. These fractionation results are compared relative to differing feed compositions, recovery, and flux. There was definite fractionation between organic (mostly soluble lignin) compounds. The average molar mass of the organic compounds in the permeate remained around 1000 g/mol; however, they ranged from 1500–4000 g/mol in the retentate. In contrast to the TOC, there was no rejection of sodium ions by the membrane (a desirable objective.) With respect to flux decline, the primary form of resistance (>99%), causing significant permeance decline, was a gel/deposition layer formed on the membrane surface. However, this could be flushed away with periodic rinses using water and/or 0.1 M NaOH. After operation at a cumulative filtration load of $\sim$4.9 Mg/m^2 with various soluble lignin containing streams, 70% of the membrane's virgin pure water permeance could be recovered by a more vigorous

Received 17 August 2007, Accepted 4 November 2007
Address correspondence to John Pellegrino, Department of Civil, Environmental, and Architectural Engineering, University of Colorado, Boulder, CO 80309-0428 Tel.: 303 735 2631; Fax: 303 492 7317; E-mail: john.pellegrino@colorado.edu

cleaning with 0.1 M NaOH including soaking and permeation. Our results seem very consistent with those previously observed for membrane applications within the pulp and paper industry.

Keywords: γ-Alumina, biorefinery, lignin, ultrafiltration, total organic carbon

INTRODUCTION

The most sustainable feedstocks for bioethanol production are lignocellulosic biomass, such as low-cost residues and wastes from agricultural processes like corn stover (1)—of which 60–80 million dry tons per year are available for ethanol production in the United States (2). Corn stover is predominantly composed of cellulose, hemicellulose, and lignin. Hemicellulose and lignin provide a protective sheath around cellulose, which must be chemically or biologically removed before cellulose-hydrolysis can occur to provide sugars for bioethanol production (3). Each type of feedstock used to make ethanol requires some form of pre-treatment to minimize the degradation of the substrate and maximize the sugar yield (3). The pre-treatment for the corn stover feedstock in this study was a novel extrusion reactor design (4), which involves sequential additions of a strong acid, such as sulfuric acid, and a strong alkaline agent, such as sodium hydroxide. The effluent from the latter stage contains a variety of lignin species, excess alkalinity, and dissolved carbohydrates—somewhat similar to the black liquor produced in the pulp and paper industry (PPI) (see Table 1). To make a lignocellulosic-biorefinery more economical and ecologically balanced, we are studying cost-effective processes to recover potentially valuable byproducts, minimize chemical consumables, and recycle water.

The filtration work we performed had two goals. One was to ascertain the fractionation that would be obtained by an inorganic membrane that might be useful for both the elevated temperature basic (the current focus) and acidic (future work) streams produced by the developing pre-treatment process. The second goal was to operate the ultrafiltration process in a small-scale production fashion in order to produce a permeate useful for subsequent studies. This latter aspect has allowed us to benchmark how robust the membrane's separation characteristics were to "imperfect" cleaning protocols.

There are four primary figures-of-merit investigated in this study: permeance decline, total organic carbon (TOC) fractionation, Na^+ recovery in the permeate, and the average molar mass of organic compounds retained and permeated through the membrane. The permeance decline was monitored to determine the degree of reversible (concentration polarization and surface, or gel, layer) and irreversible fouling (pore and surface adsorption) that occurred due to prolonged filtration and changing feed compositions. The TOC fractionation corresponded to the amount of relatively large molar mass organic species retained by the membrane, and the Na^+ recovery

Table 1. Composition of liquors in this study (liquor 0, 1, and 2) and raw black liquor (8)

	Liquor 0	Liquor 1	Liquor 2	Raw black liquor (8)
Feedstock	Corn stover	Corn stover	Corn stover	Straw
Pre-treatment by biorefinery or mill	Centrifugation	Centrifugation	Pressure filtration	200 mesh filtration
Dynamic viscosity ($Pa \cdot s$) $\times 10^{-3}$	n.a.	1.16	1.06	n.r.
Conductivity ($\mu S/cm$)	13390	13180	14340	n.r.
pH	7.9	7.7	12.2	11
Total suspended solids content (g TSS/L)	21	7.4	1.5	n.r.
Total solids (g TS/L)	47	31	18.9	82–92
Lignin content (g/L)	n.a.	n.a.	n.a.	26
TOC content (g TOC/L)	10.2	11.1	5.76	n.r.
Sodium content (g Na^+/L) (from IC)	n.a.	4.8	5.2	18–24 (from total ash)
Molar absorptivity at 274 nm (L/g/cm)	25.5	24	35	n.r.
Average molecular mass (g/mol)	1700	1800	2200	30000–60000 +

n.a. = not determined; n.r. = not reported.

represented the amount of it in the initial feed not sequestered in the retentate (for example, as Na^+ salts of organic acids). The average molar mass of organic compounds retained and permeated by the membrane was determined by using their ultraviolet (UV) absorbance and molar absorptivity at 274 nm.

Background

There have been many recent studies (5–16) conducted on membrane separation processes to recover chemicals and water in the PPI, much like what is desired in a lignocellulosic-biorefinery. In addition, early PPI application research and commercial installations stretch back to the late 1960s and are quite comprehensively enumerated by Wallberg, Jönsson and co-workers, in ref. (10). More recently, new membrane materials, both polymeric and inorganic, have become available that have a broader range of pH, solvent, and temperature stability and have been evaluated at higher temperatures for hemicellulose and lignin (12–14) recovery from alkaline liquors.

An early study conducted by Hill and Fricke (5) examined the efficacy of using polymeric ultrafiltration (UF) membranes to fractionate lignin from softwood kraft black liquor (KBL). They investigated the molar mass of fractions retained and permeated (using the ultraviolet absorbance and molar absorptivity, similar to this work) versus the nominal molar mass cutoff (MWCO) of the membrane. A nanofiltration-like membrane (MWCO $\leq$ 500 g/mol) was apparently required to retain all the phenolic components. A similar fractionation study with polysulfone polymeric membranes with cutoffs ranging between 4 and 20 kg/mol was also performed by Wallberg et al. (10). They reported 80% retention of lignin with the 4 kg/mol UF membranes and insignificant retention of sodium and sulfur (an objective), and were able to regenerate the membranes with alkaline cleaning.

In a variety of separations applications, the use of inorganic membranes is increasing, and so to in the pulp and paper industry due to their resistance to high temperatures and acidic and alkaline solutions, and potentially longer life spans. Liu et al. (8) investigated the applicability of inorganic membranes for major constituent fractionation and high flux operations in the treatment of black liquor from a straw-based pulp and paper mill. They determined that inorganic microfiltration (MF) membranes could efficiently reject most lignin and silica in the black liquor. This is of particular interest for wheat straw feed stocks that have high silica content, which can cause difficulties in alkaline recovery systems. The composition of the black liquor used in Liu et al.'s (8) experiments is summarized in Table 1 for a comparison with the solutions of interest in this study.

Wallberg et al. (9) conducted studies on the UF of softwood KBL by using an alumina-titania ceramic tubular membrane (CTM). Their work investigated the effect of temperature on the permeate flux and the percent retention of lignin and inorganic compounds. Wallberg et al. (9) found that at higher

operating temperatures the permeate flux increased and the lignin retention decreased, which is likely due to the increased solubility of lignin at elevated temperatures. The increased volumetric flux at higher temperatures is extremely advantageous for the pulp and paper industry because KBL effluent is generally above boiling. Wallberg and Jönsson and co-workers have continued studying inorganic membranes for a variety of KBL and PPI applications (11, 12, 15). These investigators noted that over a wide variety of membranes the retention of lignin compounds decreased at elevated temperatures and they also suggest that trace multivalent ions aid formation of lignin colloids that facilitate the overall lignin retention.

Many researchers have noted that the optimal membrane geometry (e.g. MWCO) for lignin fractionation targets is not always obvious due, in part, to the heterogeneity of the lignin from different sources and the "cooking" process variables. In addition, the membrane process conditions, including the mass transfer boundary layer will make a difference (for example, 10, 11, 13, 16). Among the differences between previous studies on CTM KBL filtration and this work is that our measurements were made at room temperature and the liquor is derived from corn stover. Agricultural residues such as corn stover contain lower lignin content than hardwoods (see Table 2) and other typical pulping feed stocks, such that less pretreatment is necessary to prepare the material for enzymatic hydrolysis in bioethanol production. In this work, we perform initial studies to compare results obtained with a biomass-to-fuel liquor to those from prior PPI applications in order to assess how well prior PPI benchmarks for membrane unit operations can extrapolate into the emerging biofuels/biorefinery industry applications.

EXPERIMENTAL

Materials

The pre-hydrolysis liquors used in this study were obtained from PureVision Technology, Inc. located in Fort Lupton, CO. PureVision has developed an

Table 2. Chemical composition of main components in hard Maple (hardwood) and corn stover

Main components	Hard Maple	Corn stover
Glucan (% dry weight)	42.8	36.4
Lignin (% dry weight)	25	16.6
Xylan (% dry weight)	16.8	18

Wiselogel, A., Tyson, S., and Johnson, D. (1996). Biomass feedstock resources and composition. In: C.E. Wyman (ED.) *Handbook on Bio ethanol: Production and Utilization*; Taylor and Francis, Bristol, PA. pp 105–116.

extrusion reactor design (4) that breaks down woody biomass, such as corn stover, into a cellulosic fraction (as a dense plug) and two aqueous streams, one acidic and the other basic, containing various valuable byproducts. Two batches of the latter (basic) effluent were used as the main feedstocks for this work, referred to as liquors 1 and 2. Their compositions are summarized in Table 1, along with that of an initial batch, referred to as liquor 0, which we used for preliminary studies. The pre-treatment hydrolysis process is still being optimized so the liquor composition changes depending on process modifications, such as varying the ratio of sodium hydroxide to biomass (corn stover) and the method of solids separation. For example, liquor 0 and liquor 1 were centrifuged at 40 rpm and liquor 2 was pressure filtered through a 100 μm filter. Due to the different suspended solids removal techniques, the total suspended solids (TSS) and total organic carbon (TOC) content are considerably different between these liquors (see Table 1).

Filtration Apparatus

A UF γ-alumina CTM with a nominal pore size of 5 nm and effective membrane area of $\sim 10.8\ cm^2$ was obtained from CeraMem Corporation for these experiments. It is a single tubular membrane (circular cross-section) with an ~ 0.65 cm inside diameter and ~ 5.3 cm length. The pure water permeance (PWP) through the CTM, prior to any filtrations with liquors, was approximately $2.77 \times 10^{-7}\ m^3 \cdot m^{-2} \cdot s^{-1} \cdot kPa^{-1}$. The filtration experiments were lumen fed and conducted in a batch mode, thus the retentate was recycled to the feed container throughout the experiment. The feed was delivered through high-pressure tubing (Masterflex PharMed L/S 18) into a Cole-Palmer (Masterflex) console pump. The average feed flow rates supplied by the pump during tests 1 and 2 were $8.7 \times 10^{-7}\ m^3/s$ and $9.4 \times 10^{-7}\ m^3/s$, which corresponded to average crossflow velocities through the CTM during tests 1 and 2 of 0.10 and 0.12 m/s, respectively. A back-pressure regulator, located between the membrane and retentate line, established the transmembrane pressure gradient to generate permeate. Figure 1 shows a schematic of the different components in the filtration apparatus.

Experimental Approach

For clarity, a schematic flowsheet of the experimental steps is presented in Fig. 2. Determination of the clean membrane's pure water permeance before any testing is labeled PWP 1. Prior to test 1 the effect of transmembrane pressure on the volumetric flux was determined for liquors 0 and 1 to see if a gel layer formed (Fig. 3). Following the liquor 0 filtrations, the membrane was flushed with filtered, deionized, 18 MΩ resistance water

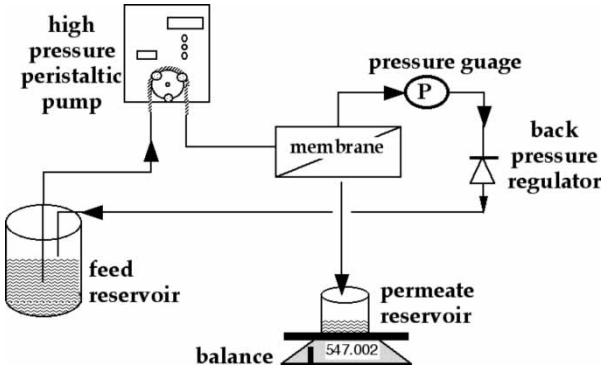

Figure 1. Filtration apparatus schematic used with γ-alumina, 5 nm, CTM.

(aka MQ water) and 0.1 M NaOH, and the new pure water permeance (PWP 2) was determined as a baseline for work with liquor 1. Following tests 1 and 2, the membrane was cleaned and the new pure water permeances (Fig. 4) of the membrane (PWP 3 and PWP 4) were measured

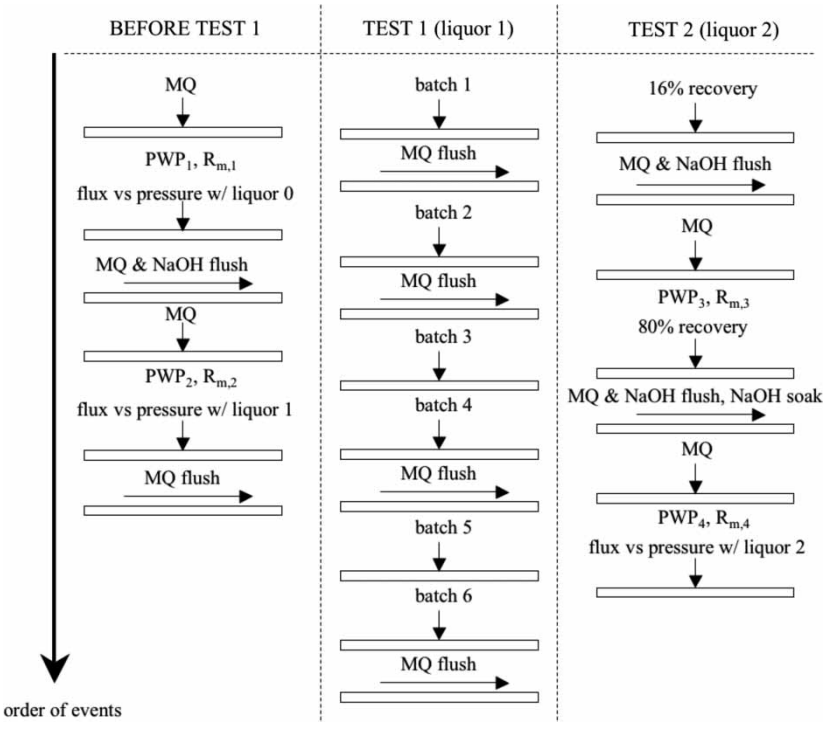

Figure 2. Schematic flowsheet of the experimental steps and protocols including cleanings and determination of filtration resistances

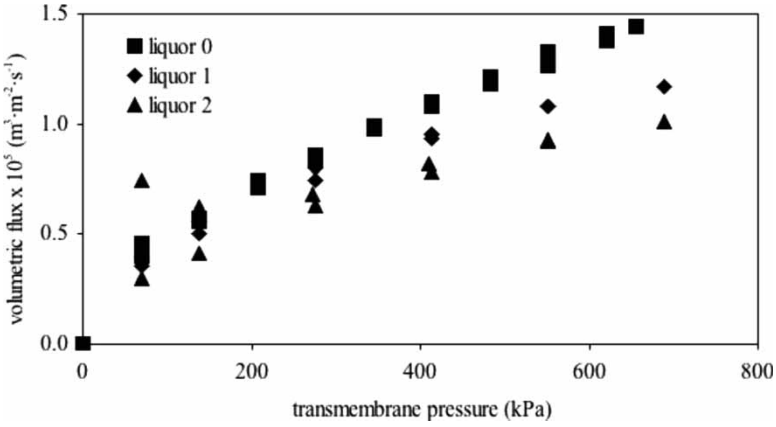

Figure 3. Effect of transmembrane pressure on the volumetric flux of liquor 0, 1, and 2 through the CTM.

to calculate the degree of irreversible fouling that occurred during the liquor filtration tests 1 and 2.

During test 1 six separate batches of ~400–700 g of liquor 1 feed were filtered at a transmembrane pressure of 552 kPa (80 psi). After approximately 50 to 70% recovery of feed as permeate (aka permeate recovery) for each batch, the test was stopped and a new batch of ~400–700 g of liquor 1 was added to the feed container and the test was resumed. Permeate was collected into pre-weighed vials, which were weighed and replaced when

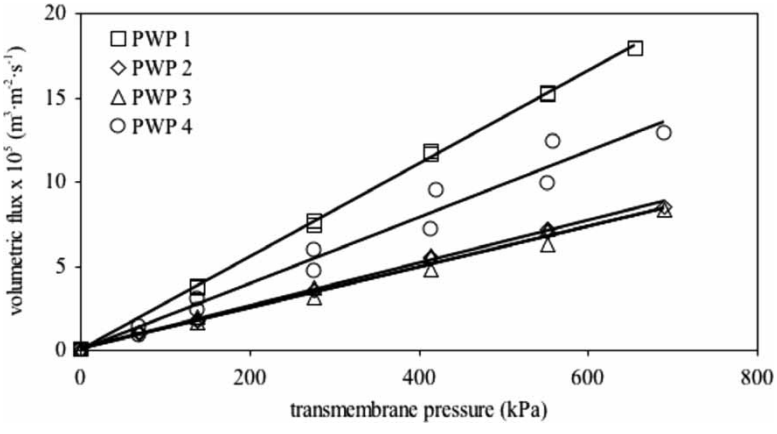

Figure 4. Effect of transmembrane pressure on the volumetric flux of pure water through the CTM; the slope of the line is the pure water permeance (PWP). PWP_1 = PWP of new membrane; PWP_2 = PWP of membrane before test 1; PWP_3 = PWP of membrane after 16% recovery of test 2; PWP_4 = PWP of membrane after test 2.

full to obtain the permeance decline trend. The retentate samples, collected after each permeate vial replacement, were obtained from the retentate line (for batches 1–4 only). The retentate flow rate was measured during each sampling time to monitor any change in crossflow velocity and to calculate the hydrodynamic boundary layer mass transfer coefficient. Following batches 1, 2, and 4 the membrane was flushed with MQ water.

During test 2, one large batch of ~4000 g of liquor 2 feed was permeated at a transmembrane pressure of 278 kPa (40 psi). Permeate was continuously weighed on an analytical mass balance (Sartorius L810) and the retentate samples were collected periodically from the retentate recycle line to monitor the same effects as described for test 1. Following 16% permeate recovery (approximately 75 h) the membrane was flushed with 0.1 M NaOH, due to a 40% drop in permeance. Following the sodium hydroxide flush, test 2 resumed and run to a total of 80% permeate recovery.

TOC and Sodium Recovery

The total organic carbon and sodium recovery were determined for batches 1–4 of test 1 and all of test 2. Total organic carbon was measured using a Sievers 800 TOC Analyzer following the method outlined in Standard Methods 5310 C (17). Potassium hydrogen phthalate (KHP) standards were used that ranged from 0 to 10 mg KHP/kg MQ water. The TOC recovery (TOC_{rec}) was determined by the mass of TOC in permeate at time t ($TOC_{p,t}$, g) divided by the mass of TOC in the feed at time 0 ($TOC_{f,0}$, g). The TOC recovery was calculated by the following equation:

$$TOC_{rec} = \frac{TOC_{p,t}}{TOC_{f,0}}. \quad (1)$$

The sodium concentration was determined using a Dionex Ion Chromatography analyzer with an IonPac CS12 (10–32) cation analytical column. Sodium chloride (NaCl) standards from Sigma-Aldrich were prepared at concentrations of 5, 10, 20, 30, 40, and 50 mg NaCl/kg MQ water. Similar to TOC, the sodium recovery was calculated by the following equation:

$$Na^+_{rec} = \frac{Na^+_{p,t}}{Na^+_{f,0}} \quad (2)$$

where the subscripts have a similar interpretation as above.

Molecular Mass of Fractionated Organic Species

An ultraviolet (UV) spectrophotometer, HACH DR/4000U, was used to determine the approximate compositional change of the lignin in the

various streams. Five-hundred-fold dilutions were performed on the feed, retentate, and permeate after 30 min of test 1, and on the feed, retentate and permeate after 80 min of test 2 to compare the UV spectra as shown in Fig. 5. Five-hundred fold dilutions were also done on all samples throughout tests 1 and 2 for UV analysis in order to compare the compositional change in the feed, retentate, and permeate by differing peak absorbances at 274 nm. This wavelength was chosen because π-π^* electron transitions occur between 270 and 280 nm on the UV spectrum range for phenolic substances (such as lignin), benzoic acids, and polycyclic aromatic hydrocarbons (18, 19). The decomposition products of lignin contain fractions of humic acid, which exhibit a featureless increase in absorbance with decreasing wavelength (20), which is also displayed in Fig. 5. Chin et al. (20) acknowledged that since many of these lignin products are precursors of humic substances, molar absorptivities may yield important clues regarding the degree of aromaticity, extent of "humification", and molecular mass of compounds that absorb UV light between 270–280 nm. In response to this relationship, Chin and coworkers (20) developed a useful correlation between the molar absorptivity of humic substances in this UV range and the high-pressure size exclusion chromatography (HPSEC) mass averaged molecular mass. A regression analysis of their data resulted in the following equation for characterizing the relationship between the molar absorptivity at 280 nm and molecular mass (20):

$$M_M = 3.99\varepsilon + 490 \tag{3}$$

where, M_M is the average molecular mass (g/mol) and ε the molar absorptivity ($L \cdot mol^{-1} \cdot cm^{-1}$) at 280 nm. This correlation has been successful for humic

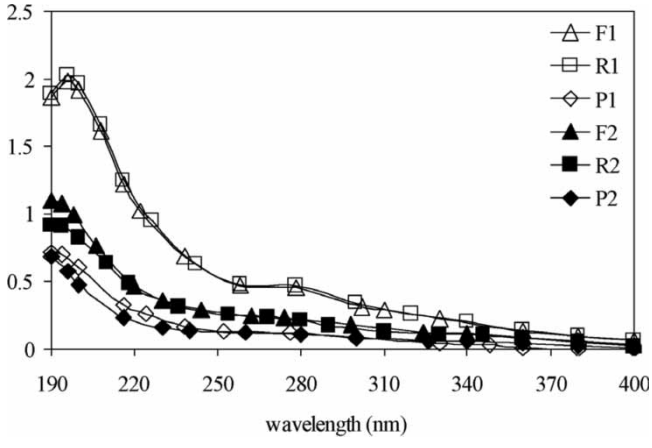

Figure 5. Ultraviolet absorbance spectra for the liquor 1 and 2 feed, retentate, and permeate at 500-fold dilution. Test 1: feed = open triangles, retentate after 30 min = open squares, permeate after 30 min = open diamonds. Test 2: feed = filled triangles, retentate after 80 min = filled squares, permeate after 80 min = filled diamonds.

substances with $M_M > 490$ g/mol in the absence of interfering chemical substances, such has metal oxides (20).

Total Suspended Solids and Total Solids

The total suspended solids (TSS) and total solids (TS) content were not monitored continuously during these experiments; however, the initial TSS and TS content of liquor 1 and 2 were determined for comparison between feeds used in other studies (5–9), for example, Lui et al. (8), is shown in Table 1. The TSS content was determined for duplicate samples by centrifugation in 12 cm radius device at 3370 rpm for 10 min. The percent total suspended solids were calculated by the following:

$$\%\mathrm{TSS} = \frac{M_s - M_{sup}}{M_s} \cdot 100\% \tag{4}$$

where, %TSS is the percent total suspended solids, M_s is the mass of sample (g), and M_{sup} is the mass of supernatant liquid (g). The total solids (TS) content of the initial liquor was determined for duplicate samples by evaporation of the liquid phase at approximately 95°C in a vacuum oven at an absolute pressure of ~20 kPa until no visible liquid remained. The percent total solids are given by the following:

$$\%\mathrm{TS} = \frac{M_{solid}}{M_s} \cdot 100\% \tag{5}$$

where, %TS is the percent total solids, M_s is the mass of sample (g), and M_{solid} is the mass of solid (g) that remained after evaporation of the liquid.

RESULTS AND DISCUSSION

Permeance Decline

The γ-alumina CTM had been used for preliminary experiments prior to the main tests, and had been cleaned. These experiments were conducted to determine the effect of transmembrane pressure on the volumetric flux of liquors 0 and 1 through the CTM (Fig. 3). (A similar experiment was conducted with liquor 2 after test 2.) As the transmembrane pressure increased, the higher volumetric flux caused compression of accumulated lignin particles on the membrane surface. The membranes's PWP was determined after the initial experiment with liquor 0 as $1.28 \times 10^{-7}\ \mathrm{m^3 \cdot m^{-2} \cdot s^{-1} \cdot kPa^{-1}}$, which was ~46% of its "virgin" pure water permeance. At this point experiments with liquor 1 began.

The permeance of liquor 1 (at $\Delta P_{tm} = 552$ kPa) during the flux versus ΔP_{tm} experiment (described above), and the permeance decline of liquor 1 (test 1) at $\Delta P_{tm} = 552$ kPa is shown in Fig. 6 for all six batches individually run to 50–70% permeate recovery. The permeance of liquor 1 never approached a steady-state, either overall, or within any individual batch. It dropped from $\sim$2.1 to 0.65 ($\times 10^{-8}\ m^3 \cdot m^{-2} \cdot s^{-1} \cdot kPa^{-1}$) over the entire course of permeating $\sim$1952 g—this corresponded to $\sim$1802 L/m^2 of membrane in the six batches. Following batches 1 and 2 the membrane was flushed with MQ water. The initial solution permeance in batch 2 was approximately the same as the initial solution permeance of batch 1; however, a subsequent MQ flush following batch 2 did not regenerate the membrane permeance as shown in Fig. 6. After batch 4 the membrane was flushed with MQ water and 0.1 M NaOH and the membrane permeance increased $\sim 1.4\times$ higher than at the end of batch 4. Since our experimental protocol was a batch recycle, the lack of steady state is consistent with continuous accumulation of macromolecules from an increasingly more concentrated feed stream.

The permeance decline of liquor 2 (test 2) at $\Delta P_{tm} = 278$ kPa is shown in Fig. 7. As before, loss of permeance was continuous with accumulation of unpermeated species, only punctuated by cleaning and operating perturbations, as follows. Following 16% permeate recovery (and a 40% drop in permeance) the membrane was cleaned with 0.1 M NaOH. The cleaning procedure entailed a 45 min flush with MQ with roughly 85 mL of permeation at 278 kPa, followed by 2.5 h of a 0.1 M NaOH flush with no permeation. As seen in Fig. 7, the membrane permeance was not fully regenerated by this

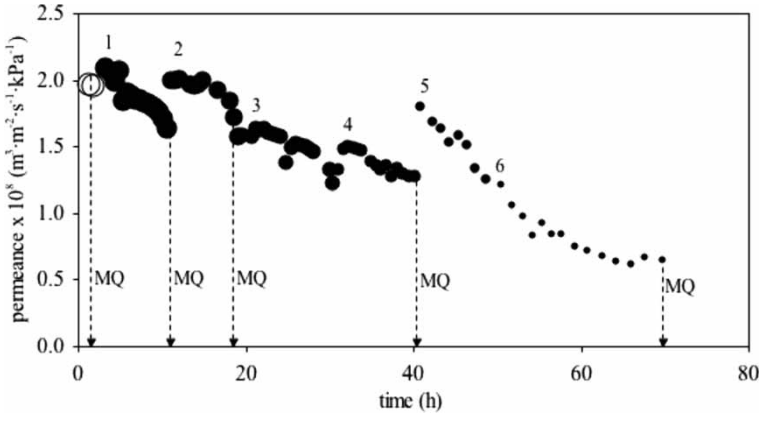

Figure 6. Permeance decline for batches 1–6 for test 1. The membrane was flushed with MQ water following batches 1, 2, 4, and 6. The permeance with liquor 1 at 552 kPa during the flux versus ΔP_{tm} test (Fig. 3) = large open circles and the data for batches 1–6 are labeled and use filled circles of decreasing size.

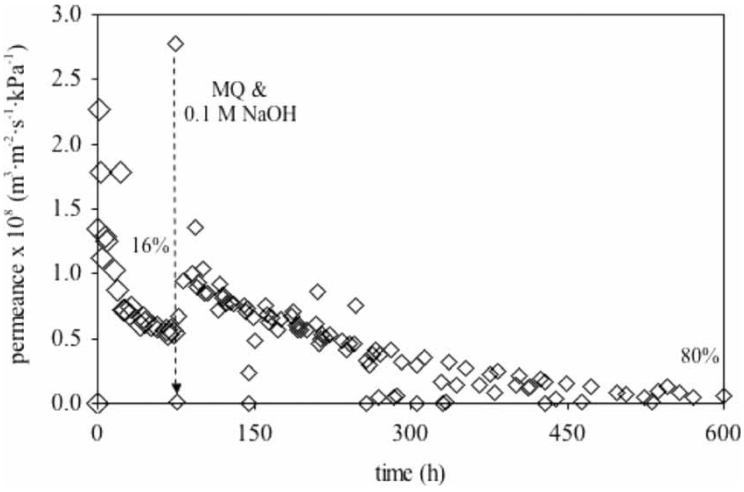

Figure 7. Permeance decline for test 2. The membrane was cleaned following approximately 16% recovery of permeate to regenerate the membrane. The first 16% recovery = larger open diamonds and 16–80% recovery = smaller open diamonds.

cleaning procedure. After determining a new pure water permeance ($1.23 \times 10^{-7}\ m^3 \cdot m^{-2} \cdot s^{-1} \cdot kPa^{-1}$), the filtration of liquor 2 was resumed and carried out to an overall 80% permeate recovery.

When varying total feed masses are used, as was done in this study, the relationship between permeance decline and the total mass permeated is a more meaningful basis of comparison than using filtration time or % recovery. Figure 8 shows the effects on flux decline from feed composition—the starting composition is "reset" to the initial value with the different batches of liquor 1 test (not so with liquor 2 test), as well as the composition of test 2 being different overall—and the total mass permeated. Following each batch of the liquor 1 test the permeance was not fully generated and the same observation was made for the liquor 2 test. Although the permeance of the first three batches of test 1 are considerably different from test 2, the fifth batch has a very similar permeance decline trend and magnitude as the beginning (the first 400 g of liquor 2 permeated) of test 2 despite the differing feed compositions and pressures used.

We will see that these results are somewhat consistent with the occurrence of adsorption in and on pores, insofar as the irreversible part increases as the total mass permeated increases, due to more adsorbed/aggregated species accumulating in hard-to-clean inner spaces. The overall decrease in permeance is also representative of the increasing mass of a deposition (or gel) layer from successful filtration. The presence of a surface gel/deposition layer is supported by Fig. 3 which shows that with increasing transmembrane

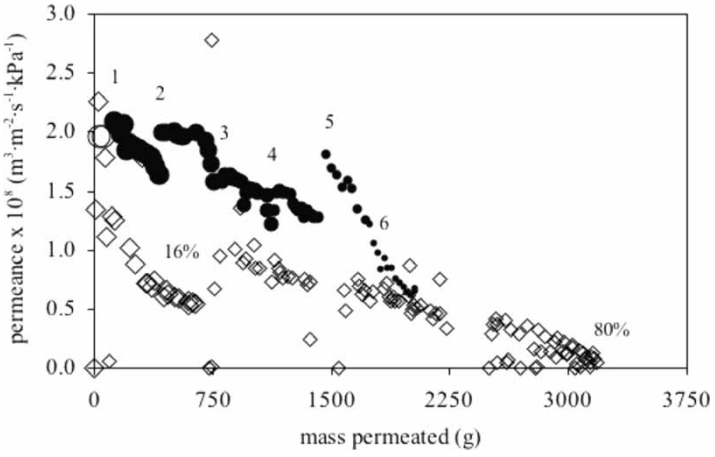

Figure 8. Permeance decline versus mass permeated for tests 1 and 2. For test 1 the batches are identified as follows: data from flux versus ΔP_{tm} test with liquor 1 at 552 kPa = larger open circles; batches 1–6 are labeled and use filled circles of decreasing size. For test 2, the first 16% recovery = larger open diamonds and 16–80% recovery = smaller open diamonds.

pressure the volumetric flux of liquor 0, 1, and 2 slowly approaches a constant, maximum value. This maximum flux decreases respectively with liquor 0, 1, and 2 due to irreversible fouling that has occurred inside the membrane prior to and during tests 1 and 2 (Fig. 3). It is important to note that a constant value was *not* reached, thus we cannot insist that a gel-layer was formed during these experiments, but the form of the flux versus pressure data is consistent with the "weak form" of critical flux (21, 22).

Vela et al. (23) conducted membrane characterization tests with a ZrO_2-TiO_2 CTM with a nominal pore size of 4 nm and a surface area of 35.5 cm^2 using solutions of 35 kg/mol polyethylene glycol (PEG). Their experiments were conducted at a transmembrane pressure of 300 kPa and several crossflow velocities (1–3 m/s.) The steady-state permeance obtained by Vela et al. (23) at 300 kPa and 1 m/s crossflow velocity was $3.7 \times 10^{-8}\ m^3 \cdot m^{-2} \cdot s^{-1} \cdot kPa^{-1}$, which is $\sim 2.5\times$ higher than the permeance obtained during batch 1 of test 1 and $8\times$ higher than the permeance obtained during the early stages of test 2. Test 2 and Vela et al.'s (23) experiments were run at similar pressures (278 kPa and 300 kPa), however, the early stage permeance obtained during test 2 was drastically lower than Vela et al. (23). They concluded that their flux decline was primarily due to gel-layer formation; this is not strictly the case in the lignin filtration process, but we can conclude that the intrinsic resistance per unit mass of the lignin surface deposition is significantly greater than that for the PEG.

Fouling Mechanisms and Resistance

During UF experiments there are three primary flux reduction mechanisms (which are all exacerbated by concentration polarization): osmotic pressure, gel-layer formation, and adsorption of solutes on the membrane surface and in the membrane pores (23, 24). However, during the UF of macromolecular solutions, the osmotic pressure can often be considered negligible (25). The flux decline viewpoint used in this study was a combination of the osmotic-pressure-adsorption model used by Ko et al. (24) and the gel-polarization model developed by Porter (25). Although a classic gel-layer may not have formed during these experiments, a deposit-layer and pseudo-gel-layer have similar growth mechanisms and effects on mass transfer. Thus, the gel-layer resistance term was added to the equation used by Ko et al. (24) as an additional layer of resistance that contributes to the flux decline from the solutions used in this study.

It is important to note that what we calculate as the R_g (resistance of a gel layer) is everything that can be washed away by the MQ water (and/or NaOH) flush made prior to measurements of pure water permeance. Thus it may incorporate several types of aggregated material.

Concentration polarization is the increase in concentration of colloidal and macromolecular material in a layer adjacent to the membrane surface. This can then increase surface and pore mouth adsorption processes, as well as, lead to a phase change, or gel formation. UF membranes are exceptionally prone to this latter form of fouling, especially when they are used to separate macromolecular solutions that can self-associate, during which flux decline can occur in seconds. This avenue of fouling is considered to be reversible and can be mitigated by the crossflow velocity across the membrane surface, regular cleaning, and the use of hydrophilic or charged membranes to minimize adhesion to the membrane surface (26). All other sources of flux decline are considered irreversible, even though rigorous chemical and physical cleaning regimes may be able to remove some of the fouling material and lower the resistance afterward.

From the initial pure water permeance, the membrane's "virgin" intrinsic resistance was determined as $3.61 \times 10^{12}\ m^{-1}$:

$$R_{m,1} = \frac{1}{\eta_w PWP_1} \tag{6}$$

where, $R_{m,1}$ is the membrane's intrinsic resistance (m^{-1}), PWP_1 is the pure water permeance ($m^3 \cdot m^{-2} \cdot s^{-1} \cdot kPa^{-1}$), and η_w is the dynamic viscosity of MQ water ($kPa \cdot s$). The membrane resistance obtained experimentally by Vela et al. (23) for a ZrO_2-TiO_2 membrane was $8.9 \times 10^{12}\ m^{-1}$, which is on the same order of magnitude as the γ-alumina membrane used in this study, but somewhat higher, due to the different separation layer and larger nominal pore size of the γ-alumina CTM.

Following filtrations with MQ-water and liquor 0, and a flush with MQ water and 0.1 N NaOH, the membrane's pure water permeance irreversibly decreased to $1.28 \times 10^{-7}\ m^3 \cdot m^{-2} \cdot s^{-1} \cdot kPa^{-1}$. Using this as the pure water permeance (PWP_2) of the used membrane, the total resistance due to the membrane and an adsorbed layer ($R_{m,2}$) was determined as $7.81 \times 10^{12}\ m^{-1}$ using the same relationship as Eq. (6), but with the new values. Thus, the resistance due to adsorption within the pores (and pore plugging) was the difference between these two values $\sim 3.57 \times 10^{12}\ m^{-1}$, equivalent to another γ-alumina membrane in series.

Similarly, following test 1, the membrane was flushed with MQ water but, however, it was *not* flushed with NaOH solution, and therefore the individual contribution of irreversible fouling (adsorption) was not determined prior to test 2. However, following 16% recovery of test 2, the membrane was fully cleaned by flushing with MQ water, followed by 0.1 M NaOH. Then the pure water permeance (PWP_3) was determined as $1.23 \times 10^{-7}\ m^3 \cdot m^{-2} \cdot s^{-1} \cdot kPa^{-1}$. With this, the total resistance due to the membrane and the accumulated adsorbed layer on the membrane ($R_{m,3}$) was determined as $8.13 \times 10^{12}\ m^{-1}$ following Eq. (6).

Following test 2, the membrane was thoroughly cleaned by flushing with MQ water and 0.1 M NaOH, and soaked in the same NaOH solution for $\sim$20 h. The new pure water permeance (PWP_4) increased to $1.96 \times 10^{-7}\ m^3 \cdot m^{-2} \cdot s^{-1} \cdot kPa^{-1}$. This 37% increase in the pure water permeance was most likely due to the more thorough cleaning in which all surfaces of the membrane were in contact with the NaOH solution for an extended time. With this, the total resistance due to the membrane and the accumulated adsorbed layer on the membrane ($R_{m,4}$) was determined as $5.1 \times 10^{12}\ m^{-1}$ (again using the form of Eq. (6)).

As we performed all the filtrations, the total resistance due to the formation of a "gel" layer on the membrane surface, and the unremoved adsorbed foulants (in, on, and/or plugging pores), was calculated as a function of the flux of the liquors through the membrane using the following (24):

$$R_{T,i} = \frac{1}{\eta_{l,i} P_{l,i}(t)} \tag{7}$$

where, $R_{T,i}$ is the gel-layer resistance (m^{-1}) formed during test i, $P_{l,i}$ is the permeance of liquor i through the membrane ($m^3 \cdot m^{-2} \cdot s^{-1} \cdot kPa^{-1}$) as a function of time, and $\eta_{l,i}$ is the dynamic viscosity of liquor i determined with a Cannon-Fenske routine viscometer. For liquors 1 and 2 the viscosities were 1.16×10^{-6} kPa · s and 1.06×10^{-6} kPa · s (at 20°C), respectively.

The total resistances and the various membrane filtration resistances are plotted in Figure 9. $R_{m,1}$ is the virgin membrane's resistance and $R_{m,2}$ is the first value of a dirty membrane's resistance after flushing away the reversible fouling. These numbers were obtained with pure water filtration. Over the

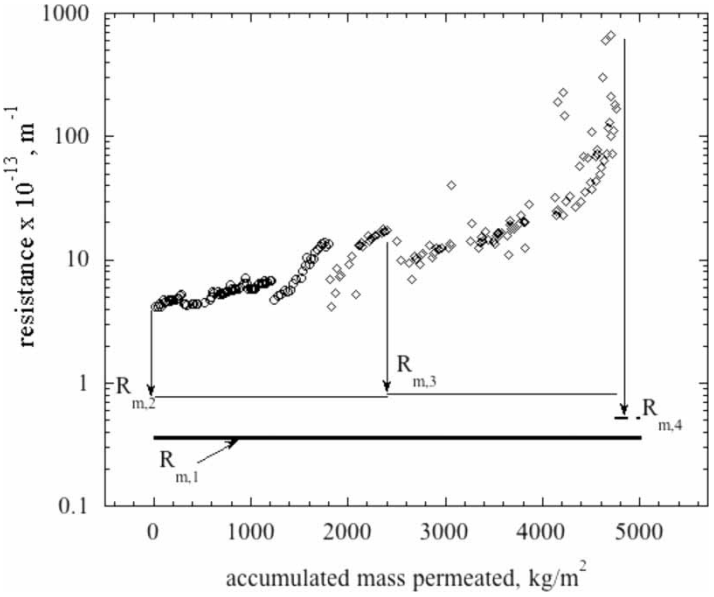

Figure 9. Total filtration resistance versus the accumulated mass per unit area permeated. The horizontal straight lines indicate new membrane's resistance ($R_{m,1}$) and the various "dirty" membrane resistances ($R_{m,1}$, $R_{m,3}$, $R_{m,4}$) measured at the points indicated by the vertical arrows.

ensuing period of filtering $\sim$2.4 Mg/m^2 of both liquor 1 and 2 there were several water flushes performed (see Fig. 2) and the total filtration resistance maintained at a level over an order of magnitude higher than the both $R_{m,1}$ and $R_{m,2}$. At this point (after the 2.4 Mg/m^2 of permeate) a flush with both DI water and 0.1 M NaOH was followed by a PWP measurement, yielding $R_{m,3}$, which was only slightly greater than the previous "dirty membrane" value, $R_{m,2}$. Thus, we infer that the overwhelming majority ($>$99%) of the filtration resistance is due to a "flushable" surface layer (aka a "gel" layer).

The filtration of liquor 2 was continued, without any further flushes, until an accumulated total of $\sim$4.9 Mg/m^2 had been permeated. For most of that period (up to $\sim$4 Mg/m^2 of permeate) the total filtration resistance stayed in the range of 10–20x the dirty membrane's value ($R_{m,3}$). Between 4 and 4.9 Mg/m^2 of permeate the total resistance increased over another order of magnitude. Nonetheless, most of this resistance was reversible upon flushing and soaking with MQ H_2O and 0.1 M NaOH, and there was indication that some of the previously "irreversibly" attached foulants had been successfully removed because the dirty membrane's resistance was now $\sim$ halfway between the virgin value and the previous dirty membrane's one ($R_{m,3}$).

In general, it appears that the intrinsic resistance the membrane provides is 0.36×10^{13} m^{-1}; irreversibly adsorbed material contributes additional

resistance between ~0.15 and 0.45 × 10^{13} m^{-1}; and reversible gel deposition provides the majority of the total resistance, on the order of 4– 20 × 10^{13} m^{-1} (during lower recoveries), and up to >600 × 10^{13} m^{-1} at very high recovery of feed as permeate.

Interestingly, high gel/deposition-layer resistance agrees with the observation made by Vela et al. (23) that ceramic membrane experiments run at lower crossflow velocities yield a surface gel layer that is the primary resistance mechanism. Lui et al.'s (8) experiments with a α-alumina ceramic tubular membranes and black liquor also concur. They observed that the gel-layer contributes approximately 80% of the total filtration resistance. (N.B. It's not clear that a gel-layer is actually formed, since its signature—flux independent of increasing transmembrane pressure—was not really determined by ourselves or the other investigators. We refer to it as a gel even though it is more likely a reversible build-up of agglomerated lignin fragments.)

Concentration Polarization

Membrane fouling due to adsorption of molecules and gel/deposition-layer formation on the membrane surface can lead to irreversible decline in membrane permeance (27). Concentration polarization is considered to be easily reversible and can be mitigated by crossflow velocity across the membrane surface to minimize the thickness of the boundary layer for mass transfer. The Reynolds number for the flow of the liquor through the lumen of the tubular membrane was calculated by the following (28):

$$\mathrm{Re} = \frac{d_h U \rho_l}{\eta_l} \tag{8}$$

where, d_h is the hydraulic diameter (m), U is the average cross flow velocity (m/s), ρ_l is the density of liquor 1 or 2 (g/m^3) at 20°C, and η_l is the dynamic viscosity ($g \cdot m^{-1} \cdot s^{-1}$) of liquor 1 or 2 at 20°C. The average Reynold's numbers during tests 1 and 2 were 602 and 781, which corresponded to laminar flow (Re < 2300). The Schmidt number (Sc), the ratio of the shear component for diffusivity to the diffusivity for mass transfer, was calculated by the following (28):

$$\mathrm{Sc} = \frac{\eta_l}{\rho_l D} \tag{9}$$

where, D is the diffusivity of the macromolecules (calculated as 0.92 and 1.01 × 10^{-10} m^2/s for liquor 1 and 2, respectively, using the Stokes-Einstein relationship the radii of gyration calculated in a later section), and the other variables were as previously defined.

Both the Sc and Re could change with time as the feed becomes more concentrated (both viscosity and density will change since these experiments were

run in batch mode.) However, these changes were ignored in the calculations herein because the viscosity of the retentate did not change considerably for our liquors, but that is a source of uncertainty for further consideration. Finally, the Sherwood number (Sh) was calculated by the Graetz-Leveque equation (29–31):

$$\mathrm{Sh} = 1.86\mathrm{Re}^{0.33}\mathrm{Sc}^{0.33}\left(\frac{\mathrm{d_h}}{\mathrm{L}}\right)^{0.33} \tag{10}$$

where, L is the filtration length of membrane (m) and other variables were previously defined. The boundary layer mass transfer coefficient is calculated by the following (31):

$$\mathrm{k_{BL}} = \frac{\mathrm{ShD}}{\mathrm{d_h}} \tag{11}$$

where, $\mathrm{k_{BL}}$ is the boundary layer mass transfer coefficient (m/s), and the other variables were previously defined. The average $\mathrm{k_{BL}}$ during tests 1 and 2 was 1.1×10^{-5} m/s and 1.42×10^{-5} m/s, respectively.

We use the classical definition of the concentration polarization coefficient for 100% retained species (31):

$$\mathrm{M} = \frac{\mathrm{c_{wall}}}{\mathrm{c_b}} = \exp\left(\frac{\mathrm{J_{vl}}}{\mathrm{k_{BL}}}\right) \tag{12}$$

where, *M* is the concentration polarization coefficient, $\mathrm{c_{wall}}$ is the concentration of the retained species at the wall of membrane (mol/L), $\mathrm{c_b}$ is their concentration in the bulk solution (mol/L), $\mathrm{J_{vl}}$ is the volumetric flux of liquor 1 or 2 through the membrane ($\mathrm{m^3 \cdot m^{-2} \cdot s^{-1}}$), and $\mathrm{k_{BL}}$ is as defined above. The average concentration polarization coefficient during tests 1 and 2 was 1.99 and 1.09, respectively. These values vary over a range of 16% and 21% for tests 1 and 2, respectively, during the full course of the filtrations. Thus, conditions exist for development of a gel/deposition layer, especially during the earliest stages of the filtration when the flux is the highest.

TOC and Sodium Recovery

TOC analysis was used as the measure of rejection of all organic species during these experiments. The dashed (45°) line displayed in Fig. 10 depicts zero selectivity or separation factor of a particular species through the membrane, i.e. no rejection or enhanced transport. The TOC data points are below this line so the some organic compounds were rejected by the membrane. Wallberg et al. (9) obtained similar results with an alumina-titania CTM during KBL batch filtrations with respect to the retention of lignin compounds and the sodium ions in the retentate. (N.B. Ref. 9 is not the only study conducted on these figures-of-merit, we are just using it as a

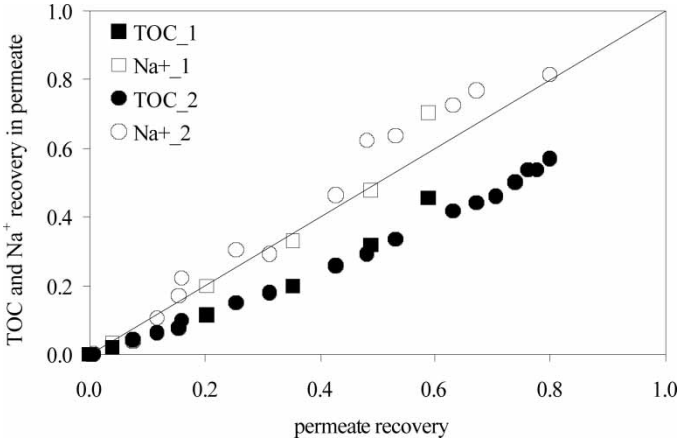

Figure 10. TOC and sodium ion recovery in permeate for tests 1 (batches 1–4) and 2. TOC for test 1 = filled squares, TOC for test 2 = filled circles, sodium ion for test 1 = open squares, sodium ion for test 2 = open circles, non-selective transference (no fractionation) = diagonal line.

convenient recent benchmark for our current work.) The TOC retention (aka "recovery" in (9)) was calculated by the following:

$$\mathrm{TOC_{ret}} = \frac{(1 - \mathrm{VR})\mathrm{c_{r,VR}}}{\mathrm{c_{f,0}}} \tag{13}$$

where, $\mathrm{TOC_{ret}}$ is the TOC retention in the retentate, VR is the volume reduction or permeate recovery, c_r is the concentration of TOC in the retentate at VR (g/L), and $c_{f,0}$ is the initial concentration of TOC in the feed (g/L). The TOC retention and permeate recovery for tests 1 and 2 are presented in Fig. 11. The TOC retention results is more similar between test 2 and (9), due to the similar permeate recoveries.

The lignin concentration in (9) was determined by Beer's law using the UV absorption at 280 nm and the molar absorption constant of 24.8 L/g/cm. The TOC content and UV absorbance was also used in our study to determine the molar absorptivity, thus it is rational to compare the TOC concentration rejected in our study with the lignin rejected in (9). As shown in Fig. 12, the trend of TOC and lignin concentration in the retentate in our study increases similarly as (9), especially during test 2, but the concentration of lignin in the retentate (9) is generally ten times higher than the concentration of TOC in the retentate in our study due to the different initial concentrations.

The other objective of our study was to recover the sodium, which would be recycled back to the lignocellulose pre-hydrolysis step as sodium hydroxide following another concentration process. As seen in Fig. 10, the general trend

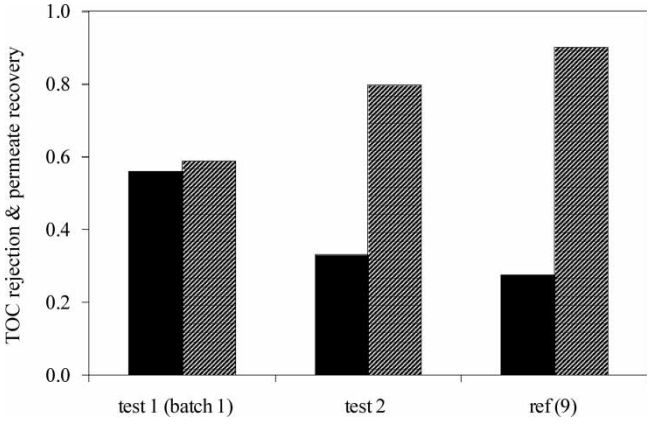

Figure 11. TOC retention and permeate recovery comparison for tests 1 (batch 1) and 2, and ref. (9). Only batch 1 from test 1 shown for clarity. Black bars = TOC rejection, crosshatched = permeate recovery.

of sodium recovery in the permeate samples shows almost complete permeation. Thus, sodium ions appear not to be associated with the higher molecular mass lignin fractions retained by this membrane, and are not convincingly (due to the uncertainty in the Na^+ analysis) permeated selectively. To achieve 100% sodium recovery with any membrane system, a full recycle, feed and bleed process would be required.

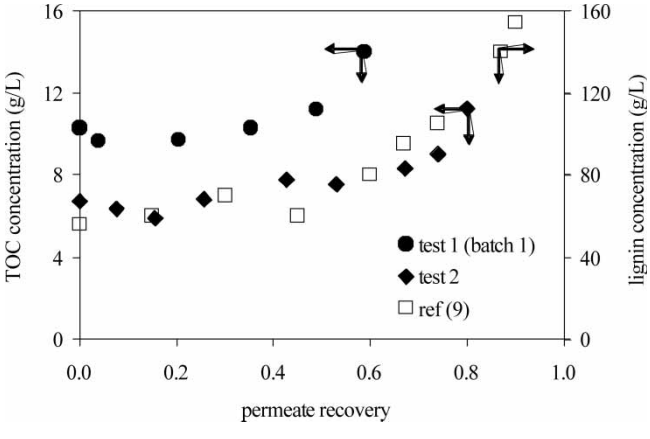

Figure 12. Retentate TOC concentration for tests 1 and 2 versus retentate lignin concentration in ref. (9). Only batch 1 from test 1 shown for clarity. Filled symbols (left-hand axis) and light symbols (right-hand axis). Test 1 (batch 1) = filled circles, test 2 = filled diamonds, ref. (9) = open squares.

Molecular Mass of Fractionated Organic Species

The molecular size and quantity of organic species retained by the membrane was determined by UV spectroscopy and literature correlations between the molar absorptivity and average molecular mass. The representative range of lignin precursors appears within the UV wavelength range of 270–280 nm. A wavelength of 274 nm was used in this study because the major peak for liquor 1 and 2 appears at this wavelength (see Fig. 5). The molar absorptivity at 274 nm was determined by the following:

$$\varepsilon = \frac{\mathrm{UVA}_{274}}{\mathrm{TOC}_{500} \cdot 12000\,\mathrm{mg/mol}} \tag{14}$$

where, ε is the molar absorptivity at 274 nm ($\mathrm{L \cdot mol^{-1} \cdot cm^{-1}}$), UVA_{274} is the ultraviolet absorbance at 274 nm at 500-fold dilution divided by the quartz cell length of 1 cm, TOC_{500} is the concentration of total organic carbon in mg/L at 500-fold dilution, and 12000 mg/mol is the molecular mass of carbon. The molar absorptivity at 274 nm for liquor 1 was $285\ \mathrm{L \cdot mol^{-1} \cdot cm^{-1}}$ ($24\ \mathrm{L \cdot g^{-1} \cdot cm^{-1}}$) and $420\ \mathrm{L \cdot mol^{-1} \cdot cm^{-1}}$ ($35\ \mathrm{L \cdot g^{-1} \cdot cm^{-1}}$) for liquor 2, respectively, as seen in Fig. 13. The molar absorptivity of liquor 1 at 274 nm agrees with the value used in (9) of $24.8\ \mathrm{L \cdot g^{-1} \cdot cm^{-1}}$ at 280 nm for chlorine-free bleached softwood liquor, which was developed by Fengel et al. (32). The permeate molar absorptivity was approximately one quarter to one half the retentate molar absorptivity for

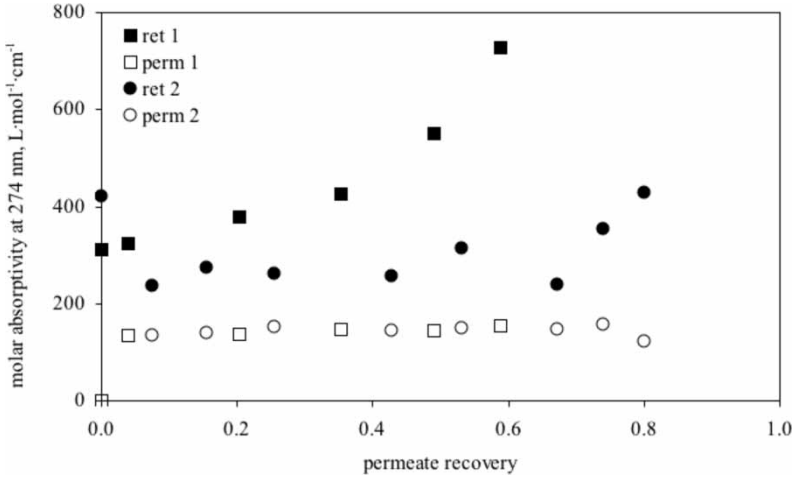

Figure 13. Molar absorptivity of organic compounds at 274 nm at 500-fold dilution of retentate and permeate for tests 1 and 2. Only batch 1 for test 1 shown for clarity. Retentate for test 1 = filled squares, permeate for test 1 = open squares, retentate for test 2 = filled circles, permeate for test 2 = open circles.

tests 1 and 2, which demonstrates that there was fractionation of organic species that absorb light at 274 nm (Fig. 13).

Using Eq. (3), developed by Chin et al. (20), the average molecular mass of organic compounds rejected and permeated by the membrane was estimated. The average molecular masses of the retentate and permeate during test 1 was 2100 and 1040 g/mol, respectively, and 1700 g/mol (retentate) and 1080 g/mol (permeate) for test 2. The different average molecular masses between the two liquors are likely due to the different initial feed compositions and the uncertainties inherent in this approach. Liu et al. (8) observed that the molecular mass distribution of KBL favored smaller molecules in more alkaline solutions, which is consistent with the smaller average molecular mass of liquor 2 (pH 12.2) in this study. During both tests the average retentate molecular mass increased considerably after 40% permeate recovery, which may be due to agglomeration of particles. The trends with permeate recovery are presented in Fig. 14.

The molecular mass of compounds in the retentate and permeate was used to estimate their radius of gyration in order to check for consistency with the nominal pore size of the CTM (5 nm). We used the following correlation from literature data (26):

$$R_G = 15.452 \cdot (M_M \times 10^{-3})^{0.7675} \tag{15}$$

where, R_G is the radius of gyration (angstroms) and M_M is the molecular mass (g/mol). The average radius of gyration of compounds that absorb light at 274 nm in the feed, retentate and permeate of test 1 are 1.8, 2.0, and 1.5 nm, and 2.0, 1.8, and 1.8 nm in test 2. The similar small size of the

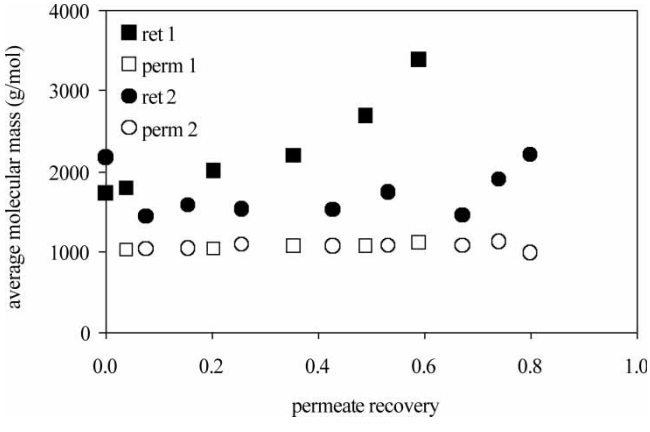

Figure 14. Average molecular mass of organic compounds of retentate and permeate for tests 1 and 2. Only batch 1 for test 1 shown for clarity. Retentate for test 1 = filled squares, permeate for test 1 = open squares, retentate for test 2 = filled circles, permeate for test 2 = open circles.

particles in the three streams is somewhat questionable since there was notable rejection observed and the nominal pore size of the CTM was 5 nm, so we consider these values rough approximations.

Despite the uncertainty in these values, the radius of gyration for the liquor 1 and 2 agrees with the study conducted by Vainio et al. (33) on dissolved KBL particles. They determined the radius of gyration of dissolved kraft lignin particles by X-ray scattering as a function of the solvent. In alkaline solutions, the phenolic hydroxyls in the lignin particles acquire a negative charge, which causes a strong electrostatic repulsion between lignin particles and only small particles form. The radius of gyration of kraft lignin in a 0.1 M NaOH solution (pH of 12.8) was approximately 1.8 nm (33), which is very similar to what we estimated for the soluble lignin in liquors 1 and 2.

γ-alumina Membrane Integrity

As mentioned in the Introduction, we are working in consort with a pre-treatment reaction process whose operating conditions have not been predetermined, and may, in fact, be influenced by the efficiency of the subsequent separation processes. This led us to begin our investigations with a commercial membrane material that promised to have robustness and desirable separation characteristics (based on the nominal pore size) for the overall application. Notwithstanding this, it is important to note that other researchers (34–36) have reported that γ-alumina forms are not completely stable in the higher pHs of liquor 2 and the 0.1 M NaOH cleaning solution.

Schaep et al. observed that γ-alumina showed corrosion at pH < 2 (34), as indicated by leaching of Al, and increases in both PWP, and nominal MWCO determined in polyethylene glycol (PEG) transport tests. Also, Van Gestel et al. created multilayer, combinations of alumina and titania NF-sized ceramic membranes, and observed that those containing weakly-crystallized γ-Al_2O_3 (and γ-AlOOH) should be restricted to $3 \leq$ pH ≤ 11 because relatively greater amounts of Al leaching was observed in their static corrosion tests (35), and the low pH effects were confirmed in dynamic tests (36) that included PEG rejection and PWP measurements.

Therefore, we performed several additional high pH exposure and nominal characterization tests, after the liquor filtration work reported herein, to assess whether membrane deterioration may have influenced our results and the conclusions drawn from them.

After the final experiment shown in Fig. 2, the CTM was flushed with 2 L of MQ water, flushed with 0.5 L of 0.1 M NaOH (∼pH 12.6) for 10 min, and then permeated with the NaOH for 5 min at 276 kPa. The membrane was then stored for 2 months in MQ water at 277 K. After this, the sequence of measurements (and results) indicated in Table 3 were done. First, we obtained the pure water permeance of the membrane, then a challenge test

Table 3. Summary of BSA filtrations for γ-alumina integrity test

Run	PWP $\times 10^7$ ($m^3 \cdot m^{-2} \cdot s^{-1} \cdot kPa^{-1}$)	BSA feed concentration (mg/L)	BSA rejection (%)	Post run cleaning step
a	2.37	1	99.4 ± 0.1	30 min MQ H_2O flush 30 min 0.1 N NaOH flush 15 min MQ H_2O flush
b	2.06	1	99.6 ± 0.2	30 min MQ H_2O flush 30 min 0.1 N NaOH flush 15 min MQ H_2O flush
c	2.36	0.5	99.4 ± 0.1	Not applicable

was done with a solution of bovine serum albumin (BSA) (at its isoelectric pH in MQ water) at the indicated concentration. Since BSA has a nominal diameter of 7 nm (37) we reasoned it be a good indicator of catastrophic damage to the nominal 5 nm pores of the γ-alumina separating layer.

The BSA solution filtrations were performed for 20 min in batch mode (retentate recycled to the feed and permeate collected) so that the BSA was being concentrated. The ΔP_{TM} was kept constant at $\sim$260 kPa and the average flux was $2-3 \times 10^{-5}$ m/s. The reported BSA rejections (defined in the classical sense $= 1 - c_{feed}/c_{permeate}$) are the average of two samplings of the feed and permeate at 10 and 20 min, whose concentration was determined by UV absorbance at 280 nm.

The results of these measurements indicated that the PWP remained lower than that for the "virgin" membrane and exhibited similar partial recovery from fouling after treatment with strong base as we observed during the liquor filtrations. The BSA rejection stayed nominally complete ($>$99.4%) which is consistent with the 5 nm separating layer remaining functionally intact. Therefore, while the long-term corrosion of this commercial γ-alumina CTM versus pH $>$ 11 may remain problematic, the filtration figures-of-merit we have reported are likely representative of the membrane's characteristics without any significant deterioration.

CONCLUSIONS

The primary form of resistance, which caused the most permeance decline during both tests, was a gel (or deposition) layer formation on the surface of the membrane. This layer's resistance was 10–20x times greater than the membrane and the persistently-adsorbed layer's resistance, and accounted for $>$99% of the total resistance, but could be removed with a simple flush of water and/or 0.1 M NaOH. It was found that a more rigorous cleaning protocol with NaOH, included soaking and permeation, could regenerate the

membrane's pure water permeance to within 70% of its virgin value even after permeating ~4.9 Mg/m^2 of lignin-containing solution and 3 water flushes and 3 water + 0.1 M NaOH solution flushes administered on a periodic basis.

There was fractionation between lignin species in the feed. The comparison between this study and prior work shows that batch experiments run to higher permeate recovery yield lower TOC retention. This implies that lignin fractionation with membranes that have 4–5 nm pores is not strictly based on steric or size considerations. Perhaps, the gel/deposition layer is acting as a dynamic membrane layer. This remains for further study. In contrast to the TOC, the concentration of sodium ions in the retentate and permeate were equal, thus there was no notable retention of sodium ions by the membrane.

The size of lignin compounds in the permeate remained fairly constant in both liquors and test modes. The average molecular mass of organic compounds in the retentate appeared to change with recovery but, interestingly, increased 24% for liquor 1 and decreased 23% for liquor 2. This may be due to the different initial viscosities of liquors 1 and 2 (higher for liquor 1), which may imply "larger" organic compounds to start with, and subsequently "seed" the further colloidal agglomeration during the batch experiments.

The average molecular mass was used to determine an approximate radius of gyration for lignin compounds in the feed, retentate, and permeate solutions; however, lower molecular mass particles, such as these, are underrepresented by the R_G-M_M model used in this study. Although this model is not a perfect correlation for this size of particles, the average radius of gyration was notably similar to the size of lignin particles in alkaline solutions determined with X-ray scattering (33).

The key differences in the results obtained in test 1 and 2 were the average size of lignin fragments fractionated, otherwise the CTM was found to provide very consistent performance figures-of-merit. The results obtained in this study provide initial design metrics for the use of ceramic tubular membranes in lignocellulosic biorefineries for the recovery of caustic chemicals which may be recycled within the process and the fractionation of lignin compounds which are valuable byproducts. The results seem very consistent with the extensive knowledge base developed by previous research for PPI applications.

NOMENCLATURE

A_{tube}	inner cross-sectional area of membrane (m^2)
c_b	bulk solution concentration (mol/L)
c_p	permeate concentration (mol/L)
$c_{r,VR}$	retentate concentration at a certain volume reduction (permeate recovery) (mol/L)

c_{wall}	membrane wall concentration on feed side (mol/L)
D	diffusivity of humic substance (cm^2/s)
d_h	hydraulic diameter (m)
J_{vi}	volumetric flux of liquor 1 or 2 ($m^3 \cdot m^{-2} \cdot s^{-1}$)
k_{BL}	mass transfer coefficient (m/s)
L	active length of membrane (m)
M	concentration polarization coefficient (−)
M_M	molecular mass (g/mol)
M_s	mass of sample (g)
M_{solid}	mass of solid (g)
M_{sup}	mass of supernatant (g)
$Na^+_{f,0}$	sodium concentration in feed at time 0 (g Na^+/L)
$Na^+_{p,t}$	sodium concentration in permeate at time t (g Na^+/L)
Na^+_{rec}	sodium recovery in permeate (–)
$P_{l,i}$ (t)	solution permeance of liquor 1 or 2 ($m^3 \cdot m^{-2} \cdot s^{-1} \cdot kPa^{-1}$)
PWP_j	pure water permeance of MQ water for membrane at different stages, j = 1 was the virgin membrane (see below for other j's) ($m^3 \cdot m^{-2} \cdot s^{-1} \cdot kPa^{-1}$)
r	inner radius of ceramic tubular membrane (m)
R_a	resistance due to adsorption in and on pores 1 (m^{-1})
R_a'	fraction of total resistance due to adsorbed layer (m^{-1})
Re	Reynolds number (–)
R_G	radius of gyration (Å)
R_g	resistance due to gel/deposition layer on the membrane surface (m^{-1})
R_g'	fraction of total resistance due to gel layer (m^{-1})
R_m	intrinsic resistance of clean membrane (m^{-1})
R_m'	fraction of total resistance due to membrane (m^{-1})
Sc	Schmidt number (–)
Sh	Sherwood number (–)
$TOC_{f,0}$	total organic carbon concentration in feed at time 0 (g TOC/L)
$TOC_{p,t}$	total organic carbon concentration in permeate at time t (g TOC/L)
TOC_{rec}	total organic carbon recovery in permeate (–)
TOC_{ret}	total organic carbon retention in retentate (–)
TOC_{500}	total organic carbon concentration in the stream at 500 fold dilution (g TOC/L)
TS	total solids (g TS/g sample)
TSS	total suspended solids (g TSS/g sample)
%TS	percent total solids (%)
%TSS	percent total suspended solids (%)
U	average cross flow velocity across membrane surface (m/s)
UVA_{274}	ultraviolet absorbance at 274 nm (-)

VR volume reduction (also referred to as permeate recovery)

Greek

ΔP_{tm} transmembrane pressure (kPa)
ε molar absorptivity ($L \cdot mol^{-1} \cdot cm^{-1}$)
η dynamic viscosity ($kPa \cdot s$ or $g \cdot m^{-1} \cdot s^{-1}$)
ρ density (g/m^3)

Subscripts

a adsorbed layer
b bulk
BL boundary layer
f feed
f,r retentate
f,0 feed at time 0
g gel/deposition layer
l,1 liquor 1
l,2 liquor 2
m membrane
m,j j = 1, new membrane; j = 2, membrane before test 1; j = 3, membrane after test 1 and 16% recovery of test 2; j = 4, membrane after test 2
p permeate
p,t permeate at time t
ret retentate
rec recovery
r,VR retentate at a certain volume recovery

ACKNOWLEDGMENTS

This research was undertaken with support from the NSF/IURC for Membrane Applied Science and Technology at the University of Colorado. We also are grateful to Dr. Richard Higgins of CeraMem Inc. for supplying membrane samples and helpful discussions.

REFERENCES

1. Glassner, D. and Hettenhaus, J. (1997) Enzyme hydrolysis of cellulose: Short-term commercialization prospects for conversion of lignocellulosics to ethanol. Report to the Biofuels Program, National Renewable Energy Laboratory: Golden, CO.

2. Kadam, K.L. and McMillan, J.D. (2003) Availability of corn stover as a sustainable feedstock for bioethanol production. *Bioresource Technol.*, 88: 17–25.
3. Hamelinck, C.N., Van Hooijdonk, G., and Faaij, A. (2005) Ethanol from lignocellulosic biomass: techno-economic performance in short-, middle- and long-term. *Biomass and Bioenergy*, 28: 384–410.
4. Wingerson, R.C. Apparatus for the separation and treatment of solid biomass. U.S. Patent application 20060283995, December 21, 2006.
5. Hill, M. and Fricke, A.L. (1984) Ultrafiltration studies on a kraft black liquor. *Tappi J.*, 67: 100–103.
6. Poddar, T.K., Singh, R.P., and Bhattacharya, P.K. (1989) Ultrafiltration flux and rejection characteristics of black liquor and polyethylene glycol. *Chem. Eng. Comm.*, 75: 39–56.
7. Bhattacharjee, C. and Bhattacharya, P.K. (1993) Flux decline analysis in ultrafiltration of kraft black liquor. *J. Membr. Sci.*, 82: 1–14.
8. Liu, G., Liu, Y., Ni, J., Shi, H., and Qian, Y. (2004) Treatability of kraft spent liquor by microfilration and ultrafiltration. *Desalination*, 160: 131–141.
9. Wallberg, O., Jönsson, A.-S., and Wimmerstedt, R. (2003) Ultrafiltration of kraft black liquor with a ceramic tubular membrane. *Desalination*, 156: 145–153.
10. Wallberg, O., Jönsson, A.-S., and Wimmerstedt, R. (2003) Fractionation and concentration of kraft black liquor lignin with ultrafiltration. *Desalination*, 154: 187–199.
11. Wallberg, O. and Jönsson, A.-S. (2003) Influence of the membrane cut-off during ultrafiltration of kraft black liquor with ceramic membranes. *Trans. IChemE*, 81: 1379–1384.
12. Wallberg, O., Linde, M., and Jönsson, A.-S. (2006) Extraction of lignin and hemicelluloses from kraft black liquor. *Desalination*, 199: 413–414.
13. Dafinov, A., Font, J., and Garcia-Valls, R. (2005) Processing of black liquors by UF/NF ceramic membranes. *Desalination*, 173: 83–90.
14. Schlesinger, R., Gotzinger, G., Sixta, H., Friedl, A., and Harasek, M. (2006) Evaluation of alkali resistant nanofiltration membranes for the separation of hemicellulose from concentrated alkaline process liquors. *Desalination*, 192: 303–314.
15. Wallberg, O. and Jönsson, A.-S. (2006) Separation of lignin in kraft cooking liquor from a continuous digester by ultrafiltration at temperatures above 100°C. *Desalination*, 195: 187–300.
16. Satyanarayana, S.V., Bhattacharya, P.K., and De, S. (2000) Flux decline during ultrafiltration of kraft black liquor using different flow modules: a comparative study. *Sep. Pur. Technol.*, 20: 155–167.
17. APHA, AWWA and WEF. (1998) *Standard Methods of Water and Wastewater*, 20th Edn.; Washington, D.C.
18. Traina, S.J., Novak, J., and Smeck, N.E. (1990) An ultraviolet absorbance method of estimating the percent aromatic content in humic acids. *J. Environ. Qual.*, 19: 151–153.
19. Braun, D.W., Floyd, A.J., and Sainsbury, M. (1988) *Organic Spectroscopy*; John Wiley: New York, 3–23.
20. Chin, Y., Alken, G., and O'Loughlin, E. (1994) Molecular weight, polydispersivity, and spectroscopic properties of aquatic humic substances. *Environ. Sci. Technol.*, 28: 1853–1858.
21. Field, R.W., Wu, D., Howell, J.A., and Gupta, B.B. (1995) Critical flux concept for microfiltration fouling. *J. Membr. Sci.*, 100: 259–272.
22. Bacchin, P., Aimar, P., and Field, R.W. (2006) Critical and sustainable fluxes: Theory, experiments and applications. *J. Membr. Sci.*, 281: 42–69.

23. Vela, M., Vincent, C., Blanco, S.A., Garcia, J.L., Gozalvez-Zafrilla, J.M., and Rodriguez, E.B. (2007) Modelling flux decline in crossflow ultrafiltration of macromolecules: comparison between predicted and experimental results. *Desalination*, 204: 328–334.
24. Ko, M.K. and Pellegrino, J.J. (1992) Determination of osmotic pressure and fouling resistances and their effects on performance of ultrafiltration membranes. *J. Membr. Sci.*, 74: 141–157.
25. Porter, M.C. (1972) Concentration polarization with membrane ultrafiltration. *Ind. Eng. Chem. Prod. Res. Dev.*, 11 (3): 234–248.
26. Baker, R.W. (2004) *Membrane Technology and Applications*, 2nd Edn.; John Wiley & Sons Ltd.: Chichester, England.
27. Sablani, S.S., Goosen, M.F.A., Al-Belushi, R., and Wilf, M. (2001) Concentration polarization in ultrafiltration and reverse osmosis: a critical review. *Desalination*, 141: 269–289.
28. Henderson, S.M., Perry, R.L., and Young, J.H. (1997) *Principles of Process Engineering*, 4th Edn.; American Society of Agriculture Engineers: St. Joseph, MI.
29. Lee, S., Amy, G., and Cho, J. (2004) Applicability of Sherwood correlations for natural organic matter (NOM) transport in nanofiltration (NF) membranes. *J. Membr. Sci.*, 240: 49–65.
30. Sherwood, T.K., Brian, P.L.T., and Fisher, R.E. (1967) Desalination by reverse osmosis. *Ind. Eng. Chem. Fund.*, 6: 2.
31. Blatt, W.F., Dravid, A., Michaels, A.S., and Nelson, L.M. (1970) Solute polarization and cake formation in membrane ultrafiltration: causes, consequences, and control techniques. In *Membrane Science and Technology*; Flinn, J.E. (ed.); Plenum Press: New York, NY., pp. 47–97.
32. Fengel, D., Wegener, G., and Feckel, J. (1981) Beitrag zur Charakterisierung analytischer and technischer Lignine. *Holzforschung*, 35: 51–57.
33. Vainio, U., Maximova, N., Hortling, B., Laine, J., Stenius, P., Simola, L.K., Gravitis, J., and Serimaa, R. (2004) Morphology of dry lignins and size and shape of dissolved kraft lignin particles by x-ray scattering. *Langmuir*, 20: 9736–9744.
34. Schaep, J., Vandecasteele, C., Peeters, B., Luyten, J., Dotremont, C., and Roels, D. (1999) Characteristics and retention properties of a mesoporous γ-Al_2O_3 membrane for nanofiltration. *J. Membr. Sci.*, 163: 229–237.
35. Van Gestel, T., Vandecasteele, C., Buekenhoudt, A., Dotremont, C., Luyten, J., Leysen, R., Van der Bruggen, B., and Maes, G. (2002) Alumina and titania multilayer membranes for nanofiltration: preparation, characterization and chemical stability. *J. Membr. Sci.*, 207: 73–89.
36. Van Gestel, T., Vandecasteele, C., Buekenhoudt, A., Dotremont, C., Luyten, J., Van der Bruggen, B., and Maes, G. (2003) Corrosion properties of alumina and titania NF membranes. *J. Membr. Sci.*, 214: 21–29.
37. Sigma-Aldrich BSA data sheet.